ELSEVIER

Journal of Power Sources 75 (1998) 73–83

JOURNAL OF POWER SOURCES

V_2O_5 xerogel lithium–polymer electrolyte batteries

Pier P. Prosini [a], Stefano Passerini [a,b,*], Raffaele Vellone [a], William H. Smyrl [b]

[a] *ENEA, C.R. Casaccia, ERG-TEA-ECHI, S. Maria di Galeria, Rome 00060, Italy*

[b] *Corrosion Research Center, Chemical Engineering and Material Science Department, University of Minnesota, Minneapolis, MN 55455, USA*

Received 23 February 1998; accepted 3 April 1998

Abstract

In this report are described the fabrication and the characterization of a lithium-metal, polymer electrolyte battery using a V_2O_5 xerogel cathode. The system operates at moderate temperatures (80–100°C). The electrochemical characterization of separate components as well as of small scale devices is also reported. The work is focused on the determination of important 'application' properties of the polymer electrolyte, i.e., the properties of the polymer electrolyte in real systems and true operating conditions. The work was developed within the ALPE (Advanced Lithium Polymer Electrolyte) project, an Italian project devoted to the realization of lithium polymer batteries for electric vehicle applications, in collaboration with the Corrosion Research Center of the University of Minnesota.

Keywords: Polymer electrolyte; Lithium battery; Vanadium pentoxide; Xerogel

1. Introduction

More than two decades of scientific and industrial research have finally made rechargeable lithium batteries commercially available on a large production scale. The batteries, commonly called lithium-ion or rocking-chair batteries, are all based on a liquid electrolyte and two intercalation electrodes. Despite the progress, the batteries are not being developed rapidly for electric vehicle applications. In fact, although the performance is extremely good for consumer market applications, especially because of the very long life (>1000 cycles), the lithium-ion battery chemistry does partially lack three of the fundamental requirements of batteries for electric vehicle application: specific energy, cost and safety. The cathode materials now used are largely responsible for all three drawbacks. Lithiated transition metal oxides ($LiCoO_2$ and $LiNiO_2$) are expensive, with a somewhat limited specific capacity (<150 mA h/g), and are not environmentally friendly. The use of a liquid electrolyte also compromises the safety of the devices. Leakage of a flammable electrolyte and the production of gases upon overcharge or overdischarge are only a few of the problems.

A somewhat 'old' battery system for electric vehicle applications [1,2] is based on the use of a polymer electrolyte in conjunction with a lithium anode and with a moderate voltage cathode (~ 3 V). Such a system has been studied for at least two decades since the introduction of polymer electrolytes [3] in 1979. However, its development has been delayed by a few problems, namely: the low ionic conductivity of the polymer electrolyte and the poor characteristics of the lithium–polymer electrolyte interface.

The first drawback arises because the operating temperature of polymer electrolyte batteries is above the ambient temperature (60–100°C). This creates the need for appropriate thermal management in order to operate the batteries. However, it must be recognized that even lithium-ion batteries for electric vehicles need thermal management and a temperature conditioning apparatus. In fact, although such batteries have a wide operating temperature range (usually from -20 to $+50$°C), their performance is affected by the temperature. In some climates, e.g., in Minnesota, the ambient temperature excursion in winter can easily exceed the operating range of the lithium-ion batteries.

The second and more stringent cause of the delay of development is determined by the characteristics of the lithium–polymer electrolyte interface. In fact, although the polymer electrolyte in contact with lithium is much more stable than any liquid electrolyte known, yet it reacts. This leads to the formation of a layer of reaction products on the lithium electrode surface. Such a layer, called passiva-

* Corresponding author. E-mail: passerin@cems.umn.edu

0378-7753/98/$19.00
PII S0378-7753(98)00094-9

tion layer, has resistive characteristics that impedes the electrode charge transfer. Thickness heterogeneity, fracture or pin holes in the passive layer, act as starting points for the growth of dendrites that can cause either battery short circuit or efficiency loss. Furthermore, the formation of the passive layer occurs at the expense of the lithium electrode, i.e., it consumes the anode.

A few years ago, it was shown that such a problem could be reduced by the addition of an inorganic filler in the polymer electrolyte formulation [4,5]. The research was initially focused on the improvement of the ionic conductivity of the polymer electrolyte through the amorphization of the polymer matrix. Successively, it has been found that some inert fillers [5] strongly improve the stability of the lithium–polymer electrolyte interface. It was also found that the characteristics of the interface were strongly enhanced by avoiding the presence of any solvent or water in the polymer electrolyte [4,6].

The present work started with this background. The investigations were focused on the synthesis and the characterization of polymer electrolytes and composite cathode films prepared by avoiding the use of any solvent. The work was initially focused on the optimization of the morphology of the starting materials, the preparation of very uniform mixtures and the formation of the polymer electrolyte and the composite cathode films [7]. As it will be shown in the following, the optimization was successful and it enhanced the electrochemical properties of the polymer electrolyte in terms of conductivity and stability of the lithium–polymer electrolyte interface. These two properties are extremely important and have to be used for a first screening of potential polymer electrolytes but, the main focus of the present report is to address the problems related to the complete lithium polymer electrolyte battery. Therefore, most of the characterizations were devoted to the interactions between the polymer electrolyte and the two electrodes.

Small scale batteries were also prepared and characterized. The choice of the cathode was vanadium oxide xerogel (V_2O_5 XRG) because of its high capacity. In previous work [8,9] it was shown that the material can intercalate up to 4 equivalents of lithium per mole of V_2O_5 at low rates ($< C/50$) and up to 2.7 equivalents at higher rates ($C/10$). The latter value corresponds to a specific capacity of 380 mA h/g and to a specific energy around 1 kW h/kg. Such high specific capacity and specific energy are, to our best knowledge, unequaled by any other cathodic intercalation compound.

The target of the work was to develop a lithium polymer battery that could be discharged in approximately 5 h or less with a delivered capacity above 150 mA h/g of active material.

2. Experimental

The polymer electrolyte and the composite cathode were prepared following the procedure described earlier [4]. Briefly, the three components of the electrolyte, polyethylene oxide (PEO) (SAF, High Purity, MW = 4,000,000), $LiCF_3SO_3$ (SAF, High purity or 3M FCC122) and γ-$LiAlO_2$ (Cyprus, HSA10), were dried in dry argon atmosphere ($H_2O < 5$ ppm) at 55, 120 and 300°C, respectively. The V_2O_5 XRG used in the composite cathode formulation was synthesized as described in Ref. [10]. The material was dried under vacuum at 100°C. The carbon added into the composite cathode (Ketjen Black, AKZO Nobel or Super P, MMM Carbon) was also dried at 120°C under vacuum.

After drying, all components were carefully sieved through 200 and 400 mesh sieves, to break or eliminate the presence of macro-aggregates into smaller powder granules. They were gently mixed in the desired proportions by ball milling for at least 12 h. The polymer electrolyte and the composite cathode compositions are shown in Table 1. The electrolyte composition was selected based on two factors, the ionic conductivity and the lithium–polymer electrolyte interfacial characteristics [6]. The composite cathode was a mixture of the active material (V_2O_5 XRG), the electronic conductor (carbon KJB or Super P), the lithium salt ($LiCF_3SO_3$) and the PEO (see Table 1). The weight fractions of the latter two components were chosen to give the same EO/Li ratio (EO: ethylene oxide unit) as in the electrolyte.

Table 1
Composition of the polymer electrolyte, the composite cathode and the composite carbon electrodes

	Electrolyte (%w/w)	Composite cathode (%w/w)	Carbon electrode (%w/w)		Carbon electrode (%w/w)
	EN20-20	VE20	CE1	CE2	CE3
PEO	70.6	29.6	73.1	73.1	80.3
$LiCF_3SO_3$	12.8	5.4	12.9	12.9	
$LiClO_4$					9.7
γ-$LiAlO_2$	16.6				
V_2O_5 XRG		55.0			
Carbon KJB			14.0		
Carbon Super P		10.0		14.0	10.0

The mixtures were hot-extruded at a temperature between 100 and 130°C as 1-mm thick, 30-mm wide ribbons. Alternatively, in the case of small quantities of mixture, the ribbons were formed by hot-pressing the mixtures in an appropriate die. The ribbons were cold-calendered to form thinner tapes. The minimum thickness of the tapes (0.05–0.1 mm) was fixed by the quality of the calendering equipment used. Thinner tapes, 0.02–0.04 mm, are obtainable since the materials have very good mechanical properties. At room temperature, a force of a few kilograms is needed to elongate and finally break a 0.1-mm thick, 30-mm wide polymer electrolyte or composite cathode tapes. The electrolyte tapes were heated at 110°C under pressure to relax the stress induced by the cold-calendering. Such a step was not necessary for the composite cathode tapes.

The geometric density (weight over volume ratio) of the composite cathode tape was 1.26 g/cm^3. This value differed from the theoretical density (1.75 g/cm^3) calculated from the density of the single components obtained by helium picnometry (Micromeritics, AccuPyc 1330). The difference in density clearly indicates the presence of void space within the composite cathode tape. The volumetric fraction of the components in the composite tapes was: $PEO_{20}LiCF_3SO_3$ 35%, carbon 6%, V_2O_5 XRG 33% and void space 27%. The polymer electrolyte tape was found to have very little void space. In fact, the geometric density was 1.49 g/cm^3 (vs. 1.57 g/cm^3 of calculated density) corresponding to a volume expansion of only 5%. Furthermore, such a volume expansion may have been due to a change in density of the polymer (PEO) as a result of the amorphization induced by the presence of the ceramic filler.

To characterize the anodic stability of the polymer electrolyte, special electrodic tapes were prepared. They were composed of PEO, one of two different lithium salts ($LiCF_3SO_3$ and $LiClO_4$) and either of two types of carbon (Ketjen Black and Super P). The weight ratios of the three components are reported in Table 1.

Throughout the whole procedure particular care was taken to avoid exposure of the material to humid air. The preparation steps were executed in controlled environments and the materials were frequently dried under vacuum at an appropriate temperature.

To characterize the above described materials, several electrochemical set-ups were used:

Conductivity	SS304/EN20-20/SS304
Anodic stability	Li/EN20-20/Composite carbon electrode
Lithium cyclability	Li/EN20-20/Li
Battery performance	Li/EN20-20/VE20

The electrochemical systems were contained either in Teflon cells with SS current collectors or in commercial 2016 coin cell cases. All cells were assembled in a dry box ($H_2O < 5$ ppm) or a dry room (R.H. < 1%). The cells were tested in an oven at 90°C.

Cyclic voltammetry experiments were performed by using a Solartron Electrochemical Interface (ECI 1287) under computer control. Low sweep rate cyclic voltammetry (< 0.1 mV/s) was performed by means of an AMEL cyclic voltammetry set-up.

Impedance measurements were performed by using a Solartron Frequency Response Analyzer (FRA1260) coupled, when needed, with a Solartron Electrochemical Interface (ECI 1287).

Galvanostatic charge and discharge cycles and reverse pulse experiments were performed by using a Maccor or an Arbin battery cycler.

3. Results and discussion

The most important characteristic of a polymer electrolyte is its ionic conductivity. In Fig. 1 is shown the conductivity (vs. $1000/T$) of the electrolyte $PEO_{20}LiCF_3SO_3 + 20\%$ γ-$LiAlO_2$ (EN20-20) prepared with the enhanced procedure described earlier. For comparison purposes, the conductivity of an electrolyte having the same composition but prepared via a less rigorous hot pressing procedure is also shown (data are taken from Ref. [6]). The data in the Arrhenius plot clearly indicate the

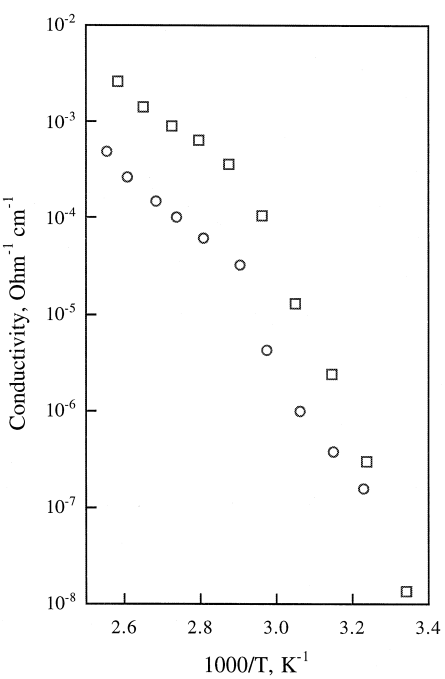

Fig. 1. Arrhenius plot (conductivity vs. $1/T$) of $PEO_{20}LiCF_3SO_3 + 20\%$ γ-$LiAlO_2$ polymer electrolyte (squares, EN20-20) obtained with the improved, dry procedure described in this work. For comparison purposes, the conductivity of the same polymer electrolyte (circles) prepared with the non-optimized process (from Ref. [6]) are also shown.

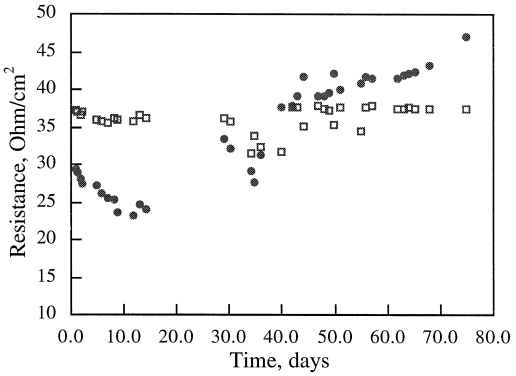

Fig. 2. Evolution of the lithium–polymer electrolyte interfacial resistance (dots) and polymer electrolyte bulk resistance (squares) of a $PEO_{20}LiCF_3SO_3 + 20\%$ γ-$LiAlO_2$ electrolyte (EN20-20) sandwiched between a lithium disc and a stainless steel electrode. $T = 90°C$.

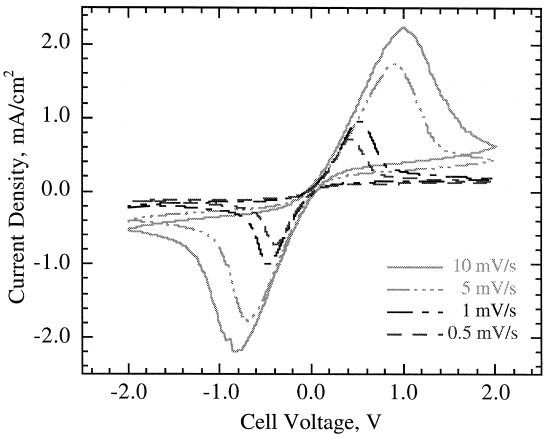

Fig. 4. Cyclic voltammetry of a $PEO_{20}LiCF_3SO_3 + 20\%$ γ-$LiAlO_2$ electrolyte (EN20-20) sandwiched between two lithium discs. Sweep rates were 0.5, 1, 5 and 10 mV/s. $T = 90°C$.

enhancement in conductivity obtained in the EN20-20 electrolyte. The conductivity of EN20-20 at 60°C (10^{-4} S/cm) exceeded the conductivity of the other electrolyte by more than one order of magnitude. Such an improvement is due to a more uniform dispersion of the components in the mixture, in particular the dispersion of the inert filler (γ-$LiAlO_2$). In fact, it is the latter component that reduces the crystalline nature of the PEO and increases the mobility of the polymer chains thereby enhancing the ionic conductivity of the polymer electrolyte [4,11]. As a result, the EN20-20 conductivity at 60°C is above 10^{-4} S/cm. Such a value is considered as a conductivity threshold above which it is possible to use the polymer electrolyte in a battery. As it will be discussed later, this threshold is a very rough estimation because it does not differentiate the cation and the anion contribution to the conductivity.

The polymer electrolyte must also be stable with the lithium anode. To investigate this issue, two different tests were performed in quasi-rest conditions and under kinetic control to simulate the lithium–polymer electrolyte inter-

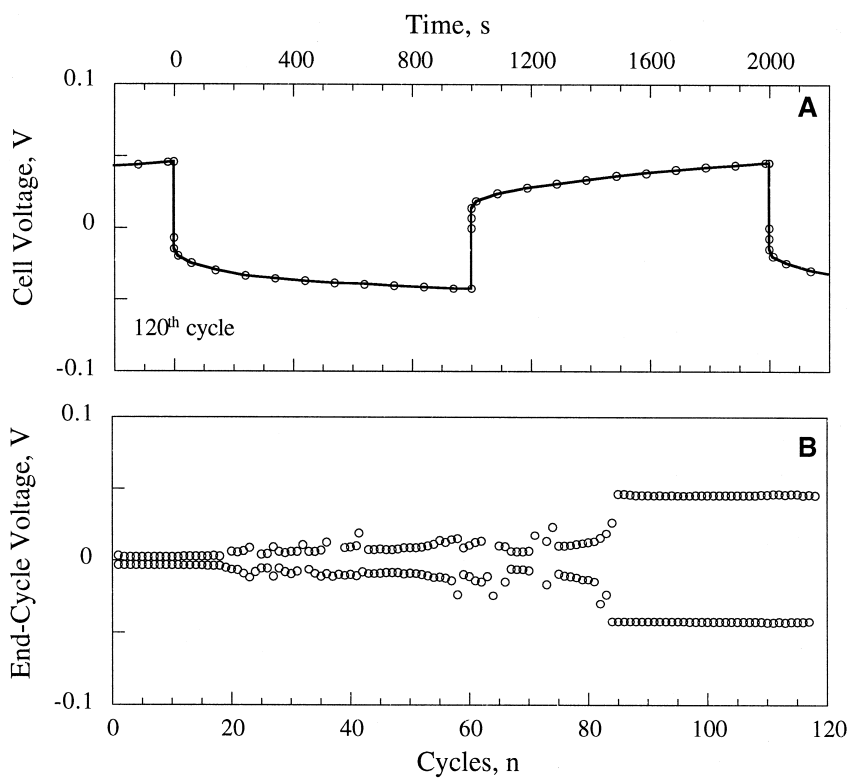

Fig. 3. Galvanostatic pulse test (±0.2 mA/cm^2) on a symmetric Li/EN20-20/Li cell. Upper plot: cell voltage behavior during the application of a pulse (120th cycle). Lower plot: end of pulse voltage evolution upon cycling. $T = 90°C$.

face behavior upon storage and operation of a lithium polymer battery, respectively.

The first characterization consisted in the determination of the polymer electrolyte bulk impedance and the lithium–polymer electrolyte interfacial impedance by means of electrochemical impedance analysis. Fig. 2 shows the evolution of the two impedances for a EN20-20 polymer electrolyte disc (0.1 mm thick) sandwiched between a lithium electrode and a stainless steel electrode. The results, taken over a period of time longer than two months, indicate a stable lithium–polymer electrolyte interface. The interfacial impedance (dots in Fig. 2) showed an initial decrease, due to mechanical improvement of the interfacial contact, followed by a slow increase, up to about 45 Ω/cm^2 after 80 days. Even more interesting is the behavior of the polymer electrolyte bulk impedance (squares in Fig. 2) that, over the same period of time, did not show any change. In the presence of a reaction between the polymer electrolyte and the lithium electrode, the bulk impedance would be expected to change with time as the result of the formation of reaction products. The constancy of the bulk electrolyte impedance can then be taken as an indirect confirmation of the chemical stability of the polymer electrolyte in contact with metallic lithium.

Fig. 3 illustrates the behavior of a symmetric cell Li/EN20-20/Li upon short galvanostatic (± 0.2 mA/cm^2; 1000 s) lithium plating–stripping cycles. The cell was constructed with a layer of polymer electrolyte 0.1 mm thick, sandwiched between two lithium electrodes. A typical cycle after stabilization (120th cycle) is shown in Fig. 3A. The cycle is symmetrical as expected from a symmetric cell that is unaffected by parasitic electrochemical or chemical reactions. In Fig. 3B is reported the cell voltage at the end of the galvanostatic pulses. In the early cycles, the cell voltage at the end of the cycles is seen to be very low, around 5 mV. The voltage/current ratio in these cycles gives a total internal impedance of 25 Ω/cm^2, in good agreement with the results obtained by impedance

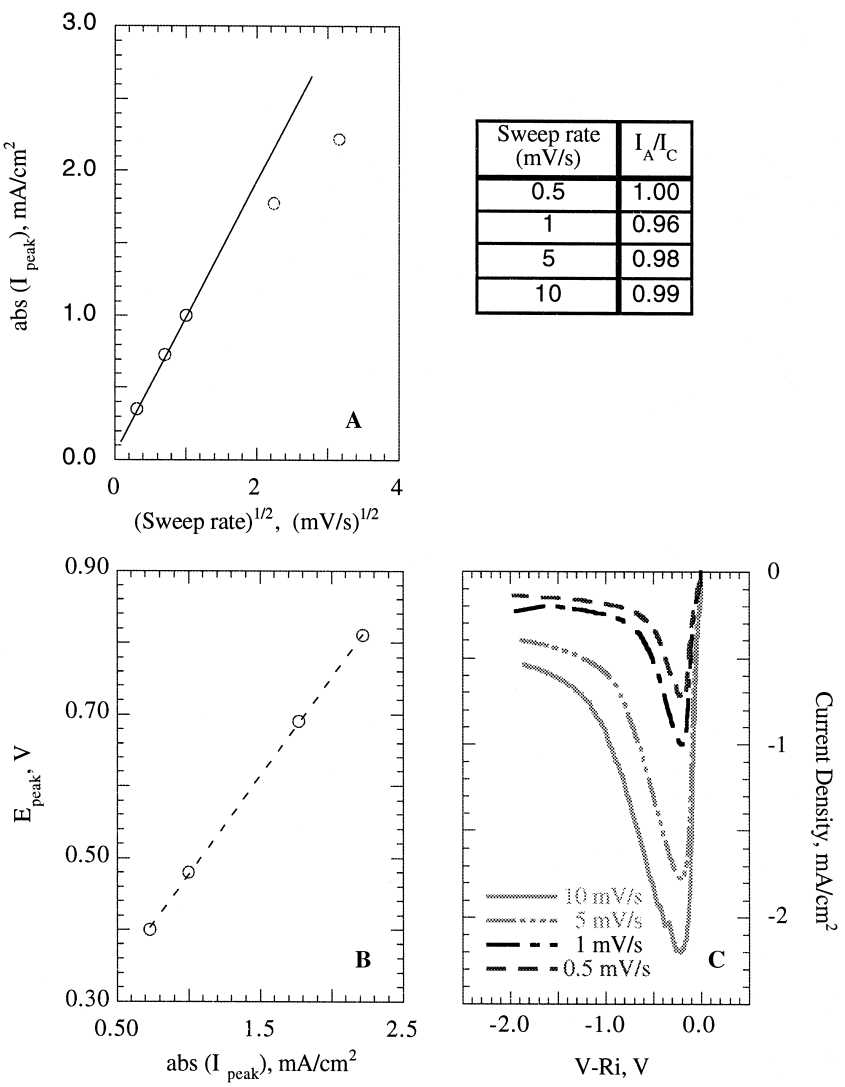

Sweep rate (mV/s)	I_A/I_C
0.5	1.00
1	0.96
5	0.98
10	0.99

Fig. 5. Elaboration of the cyclic voltammetry results shown in Fig. 4.

(see Fig. 2). Upon cycling the voltage at the end of pulse is seen to increase slowly and somewhat randomly until the 85th cycle (Fig. 3B). At this time, the end-of-pulse voltage stabilized at 48 mV corresponding to an internal impedance of 240 Ω/cm^2. The additional resistance is obviously due to the formation of a passivation layer at the lithium–electrolyte interface that is formed and destroyed, respectively during the lithium plating and stripping cycles [12]. The somewhat random end-of-pulse voltage is seen to correspond to the formation of the passivation layer. When the layer is completely formed, any further reaction is prevented or at least reduced. Similar cells were cycled for more than 500 cycles without substantial change in the cell voltage behavior. The lithium plating–stripping efficiency was measured by using a symmetric cell in which one of the two Li electrodes was a few times lighter than the other. A fixed amount of lithium was cycled back and forth in such a cell until the lithium of the thinner electrode was completely consumed by the parasitic reactions, i.e., passivation. By knowing the amount of lithium in the thinner electrode, the amount of lithium oxidized and reduced in each cycle and the number of cycles obtained, it is possible to calculate the efficiency of the lithium plating–stripping processes. Values as high as 98% have been calculated that indicate a stable lithium–polymer interface at the operating conditions, i.e., when a current flows through the electrolyte.

In Fig. 4 are illustrated the two-electrode cyclic voltammetry curves of a $PEO_{20}LiCF_3SO_3 + 20\%$ γ-$LiAlO_2$ (EN20-20) electrolyte layer sandwiched between two lithium discs. The sweep rate was changed from 0.1 mV/s to 10 mV/s. From the figure one sees that the anodic and the cathodic parts of the cycle are symmetric. The ratios of the anodic and the cathodic peak currents are very close to unity (see table in Fig. 5). As discussed in Ref. [13], a ratio of unity can be associated with a reversible or quasi-reversible process. A further confirmation is given by the behavior of the I_{peak} vs. (sweep rate)$^{1/2}$ plot (Fig. 5A) where the peak current is initially seen to increase proportionally with the square root of the sweep rate at low sweep rates (≤ 1 mV/s). At higher sweep rates (≥ 5 mV/s), a deviation from the linear correspondence is shown in the plot. Such behavior is quite common and is typical of a process that is reversible at low sweep rates and becomes irreversible at higher rates after passing through a quasi-reversible region at intermediate values of sweep rates. The transition from reversibility occurs when the relative rate of the electron transfer with respect to that of mass transport is insufficient to maintain Nernstian equilibrium at the electrode surface.

The test of reversibility with the cyclic voltammetry technique involves the satisfaction of several requirements that are related to the current peak positions (8). Unfortunately, the absence of a reference electrode in the cells under test did not permit an accurate determination of the electrode potential during the cyclic voltammetry tests. Despite the shortcomings of the procedure, we evaluated the reversibility of the cells as follows. If the anodic peak voltage is plotted vs. the peak current (Fig. 5B) a linear correlation is found. The data fall on a straight line the slope of which is assumed to correspond to the ohmic drop in the electrolyte (the assumption considers that only the electrolyte ohmic drop correlates linearly the current and the voltage). When the voltage is corrected for the ohmic drop, i.e., V–Ri instead of V is used in the plot, the peak position becomes independent of the sweep rate, as shown in Fig. 5C (anodic part). The peak separation is larger than what would be expected for a reversible process (~ 72 mV at 90°C), but is in the expected range for a quasi-reversible electrochemical reaction.

Summarizing, the cyclic voltammetry experiments showed that the lithium plating and stripping process from a polymer electrolyte has a reversible character. This confirmed the results of the galvanostatic experiments described earlier. Irreversible processes such as the reaction of the newly formed metallic lithium (plating) or lithium ions (stripping) with the polymer electrolyte, have a minor influence on the behavior of the lithium–polymer electrolyte interface.

As stated before, the conductivity of the EN20-20 polymer electrolyte allows its use in a battery at temperatures above 60°C. Nevertheless, high performance systems require the flow of very high currents through the electrolyte in the battery, even above the limiting diffusion current. As a consequence, the current flowing through the electrolyte in such circumstances cannot be sustained forever. After a certain amount of time, the overvoltage related to the establishment of a concentration gradient in the electrolyte will suddenly increase in an exponential fashion as predicted by the Sand equation [14]. The time dependent behavior has been verified experimentally on a cell consisting of a layer of EN20-20 polymer electrolyte sandwiched between two lithium electrodes. In Fig. 6 is shown the voltage evolution of such a cell during the application

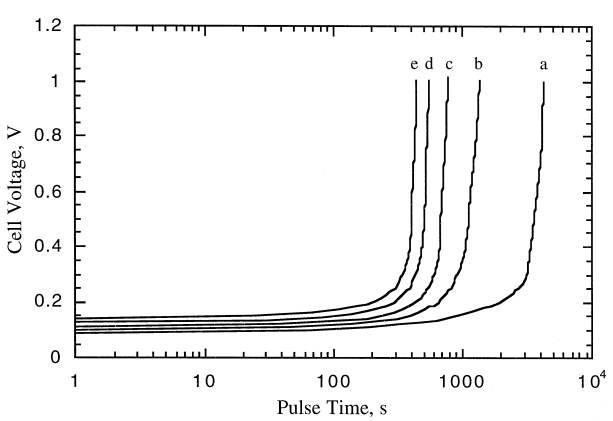

Fig. 6. Voltage behavior showed during reversal galvanostatic pulse on a symmetric Li/EN20-20/Li cell. The absolute value of the current pulses was 0.29 (a), 0.34 (b), 0.4 (c), 0.46 (d) 0.51 (e) mA/cm^2. A rest period was introduced between each single pulse. $T = 90$°C.

of constant current pulses from 0.03 to 0.17 mA/cm^2. As predicted by the Sand equation, after an initial jump due to the ohmic drop, the cell voltage stabilized and then rose steeply.

The amount of time in which the cell voltage remains stable, usually indicated with the letter τ, is expected to be proportional to the inverse of the current squared ($\tau \propto i^{-2}$). As a consequence, the amount of charge passed through the electrolyte is proportional to the inverse of the current ($Q = i * \tau \propto i^{-1}$). The latter equation can be inverted to the more useful form $Q^{-1} \propto i$. In fact, the left part of the equation yields 0 for any value of i lower than the limiting current, i.e., the limiting current can be obtained from the x-axis intercept of the Q^{-1} vs. i plot. Such a plot, obtained from the results showed in Fig. 6, is reported in Fig. 7. The data fall into a straight line with an intercept that defines the polymer electrolyte limiting current (i_L = 0.2 mA/cm^2 at 90°C). Further experiments (data not shown) indicate that τ as well as Q do not depend on the polymer electrolyte thickness, for reasonable values of the latter.

Summarizing, the galvanostatic experiments on the polymer electrolyte indicate that once the electrolyte composition and the operating temperature have been fixed, the total amount of charge that can pass through a layer of the electrolyte depends only on the selected current density (for $i > i_L$).

The stability of the electrolyte toward oxidation processes is relevant for the interface with the cathode and, is another important issue for the selection of a polymer electrolyte for battery applications. Other researcher [6] have reported oxidation stability around +5 V for polymer electrolytes with formulations similar to the present system. Their experiments were performed by applying an anodic voltage sweep to a cell consisting of a polymer electrolyte sandwiched between two smooth, inert electrodes (for example stainless steel or nickel), or between a lithium electrode (counter-electrode) and an inert electrode. The voltage was swept from the cell OCP towards more anodic values until a large current due to the electrolyte decomposition at the inert electrode interface occurred. The anodic stability limit was then taken as the onset of such a current. However, we have noted that the anodic stability of the polymer electrolyte measured in such a way is usually 1 V or more above the anodic stability of the same material in a real battery with a composite cathode. The reason for this difference lies in the fact that the anodic oxidation reaction of the polymer electrolyte in the latter occurs on finely divided carbon particles rather than on smooth electrodes. Therefore, the anodic stability measurements reported in the present work were performed by using a composite electrode, with no active material. The results obtained for a layer of EN20-20 polymer electrolyte sandwiched between a lithium electrode and a composite carbon electrode (see Table 1 for composition), are shown in Fig. 8 (Curve A). The anodic stability limit was found to be slightly above 3.8 V (vs. Li), i.e., about 1 V below the value obtained with a smooth, inert electrode [10]. The reduction of the anodic stability is certainly due to the very large contact area between the polymer electrolyte and the carbon particles

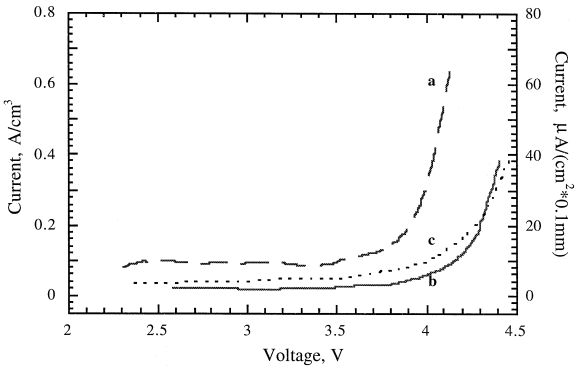

Fig. 8. Anodic voltage sweep (0.05 mV/s) of a $PEO_{20}LiX + 20\%$ γ-$LiAlO_2$ electrolyte sandwiched between a lithium disc and one of the three composite carbon electrodes. Curve a: CE1, KJB carbon and $LiCF_3SO_3$; curve b: CE2, Super P carbon and $LiCF_3SO_3$; curve c: CE3, Super P carbon and $LiClO_4$. The anion in the electrolyte always corresponded to the anion in the carbon electrode. T = 90°C.

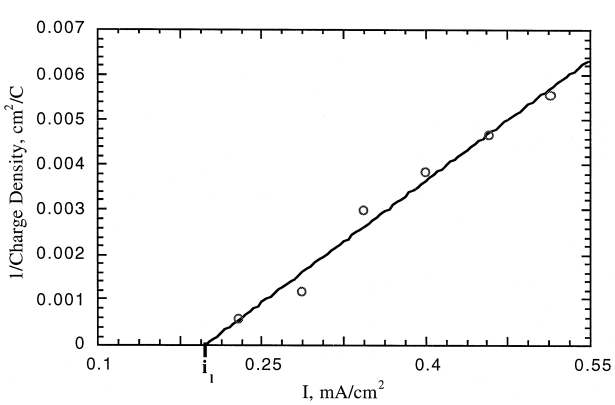

Fig. 7. Dependence of the inverse charge density (Q^{-1}) on the current density. See text for details and explanations.

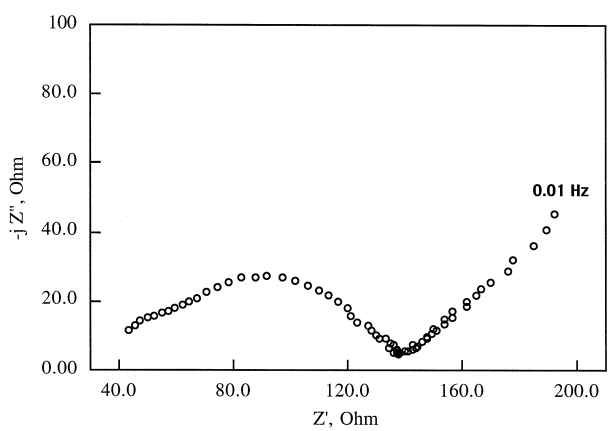

Fig. 9. Impedance spectra of the battery Li/EN20-20/VE20 after equilibration at the operating temperature (T = 90°C for 90 min).

Table 2
Circuit elements of the battery Li/EN20-20/VE20, as obtained from an impedance fit software

Polymer electrolyte	Lithium–polymer electrolyte interface		Composite cathode–polymer electrolyte interface		Composite cathode
R_{ion}, Ω/cm^2	R_{an}, Ω/cm^2	C_{an}, $\mu F/cm^2$	R_{cat}, Ω/cm^2	Q_{cat}, $\mu F/cm^2$ (n)	W_{cat}, $\Omega^{-0.5}$
60.4	17.7	0.18	167.3	18.4 (0.63)	5.6×10^{-2}

that amplifies the extent of the decomposition current at low voltage. In fact, a 0.1 mm thick composite Ketjen Black carbon electrode with a geometric area of 1 cm^2 corresponds to an approximate carbon–polymer electrolyte interfacial area of 0.6 m^2 (Ketjen Black surface area is 1250 m^2/g), i.e., 6000 times the geometric area. A further indication that the anodic stability of the polymer electrolyte is strongly related to the surface area of the carbon in the composite cathode has been found by using a lower surface area carbon (Super P: 59 m^2/g). Curve B in Fig. 8 shows the anodic sweep behavior of the EN20-20 electrolyte in contact with a Super P carbon composite electrode. The comparison of curves A and B shows that the anodic stability of EN20-20 increased by about 400 mV with carbon Super P. Unfortunately, it was not possible to compare 'chemically similar' carbons with different surface areas, so that a specific catalytic activity exerted by the different carbon samples on the anodic decomposition of the polymer electrolyte cannot be excluded.

The anodic decomposition process appeared to depend somewhat on the anion of the lithium salt of the polymer electrolyte. In fact, the substitution of the $CF_3SO_3^-$ with ClO_4^- resulted in a small change of the anodic stability limit, as showed by curve C in Fig. 8.

Summarizing, the anodic stability of the EN20-20 electrolyte in contact with Super P carbon additive in the composite cathode ($\sim$4.1 V vs. Li) is high enough to allow its use in combination with a so-called '3 V' cathodic materials but it is too low for the high voltage cathodic materials like $LiCoO_2$. Among the low voltage cathodes available, V_2O_5 xerogel was selected because of its very high intercalation capacity [8,9] ($>$ 420 mA h/g). Although the average voltage of such a cathode upon discharge is only 2.5 V (from 3.8 to 1.5 V), the delivered capacity at high rate is well above 200 mA h/g with a resulting high specific energy [9] ($>$ 500 W h/kg).

V_2O_5 XRG, lithium–polymer electrolyte batteries were formed by sandwiching one layer of polymer electrolyte EN20-20 between one lithium electrode and one composite electrode VE20. The battery stacks were then sealed in commercial 2016 coin cell. The composite cathode loading was about 0.9 mA h/cm^2 corresponding to the intercalation of 1 equivalent of lithium per mole of V_2O_5 XRG.

Fig. 9 shows the impedance spectra of such a battery, after equilibration at the operating temperature (90°C) for 2 h. With the help of software [15], three main features were fitted in the impedance spectrum (results in Table 2). A first semicircle related to the lithium–polymer electrolyte interface has an intercept at high frequency that identifies the ionic conductivity of the polymer electrolyte. The value of the capacitance (0.2 $\mu F/cm^2$) is typical of a charge transfer process at the lithium–polymer electrolyte interface [4,16,17]. The resistance associated with the charge transfer process at the lithium–polymer electrolyte interface was about 18 Ω, i.e., in a full agreement with the value obtained for symmetric Li/EN20-20/Li cells (see Fig. 2).

At lower frequencies, there is a second and larger semicircle that overlaps the first. From the high value of the capacitance (see Table 2) and the depressed shape of

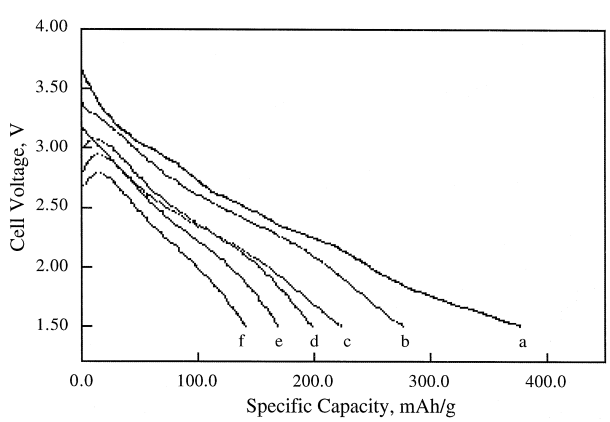

Fig. 10. Voltage vs. capacity behavior during galvanostatic discharge of the batteries Li/EN20-20/VE20. Charge current: 0.03 mA/cm^2. Discharge currents: (a) -0.03, (b) -0.06, (c) -0.09, (d) -0.12, (e) -0.15, and (f) -0.17 mA/cm^2. $T = 90$°C.

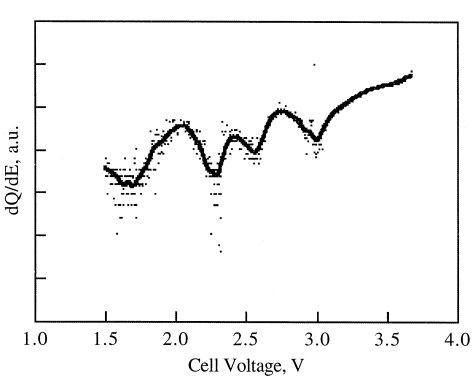

Fig. 11. Differential capacity vs. cell voltage of the Li/EN20-20/VE20. Data are obtained from results shown in Fig. 10 (curve a).

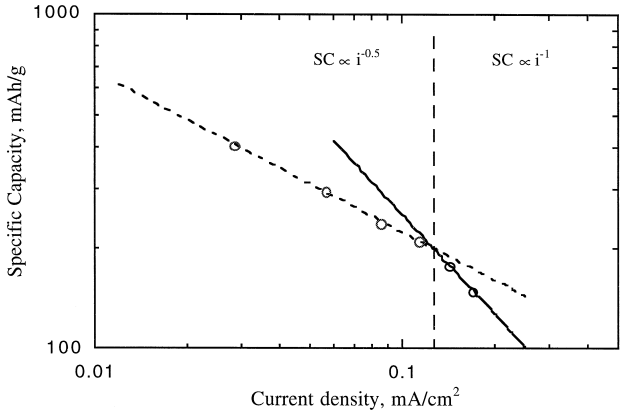

Fig. 12. Specific capacity vs. current density plot of the battery Li/EN20-20/VE20. Data are obtained from results shown in Fig. 10.

the semicircle, it is possible to assign this feature to the polymer electrolyte–cathodic material interface within the composite cathode. In fact, a 0.1-mm thick composite cathode pellet has a real surface area of the electrolyte–active cathode interface that is approximately 100 times the geometric area. The large ratio obviously boosted the double layer capacitance to the measured value reported in Table 2. Furthermore, a depressed semicircle ($n = 0.62$) was expected for a composite (porous) electrode [18]. The charge transfer resistance at the polymer electrolyte–composite cathode interface was 170 Ω/cm^2 corresponding to 17 $k\Omega/cm^2$ of active material surface area. This value is in agreement with the value obtained for V_2O_5 xerogel thin films in liquid electrolyte [19]. The high interfacial resistance could be due to a limited contact area between the polymer electrolyte fraction and the active material particles. In fact, it has been noted (see Section 2) that almost 27% of the space within the composite cathode is void.

At very low frequencies, there is a third region in which there is typical Warburg impedance behavior, related to the diffusion of lithium ions within the composite cathode.

The discharge behavior of a V_2O_5 XRG lithium polymer battery is shown in Fig. 10. The battery was discharged down to 1.5 V at various currents ranging from 0.03 to 0.17 mA/cm^2 with steps of approximately 0.03 mA/cm^2. The battery was always recharged at the lower current density (0.03 mA/cm^2).

For the active material mass loading in the composite cathodes (~ 0.9 mA h/cm^2), the discharge currents selected corresponded to an intercalation rate ranging from 0.033 equivalent of lithium per hour (Li/h) to 0.183 Li/h. At the lower discharge rate a specific capacity of almost 400 mA h/g was obtained from the battery in approximately 86 h. This result is in substantial agreement with the specific capacity of V_2O_5 XRG in liquid electrolytes [8,9]. The differential capacity vs. cell voltage (Fig. 11) obtained from the lowest rate discharge of Fig. 10, closely reproduces the typical behavior of V_2O_5 XRG reported elsewhere [19,20]. In Fig. 12, the specific capacity is

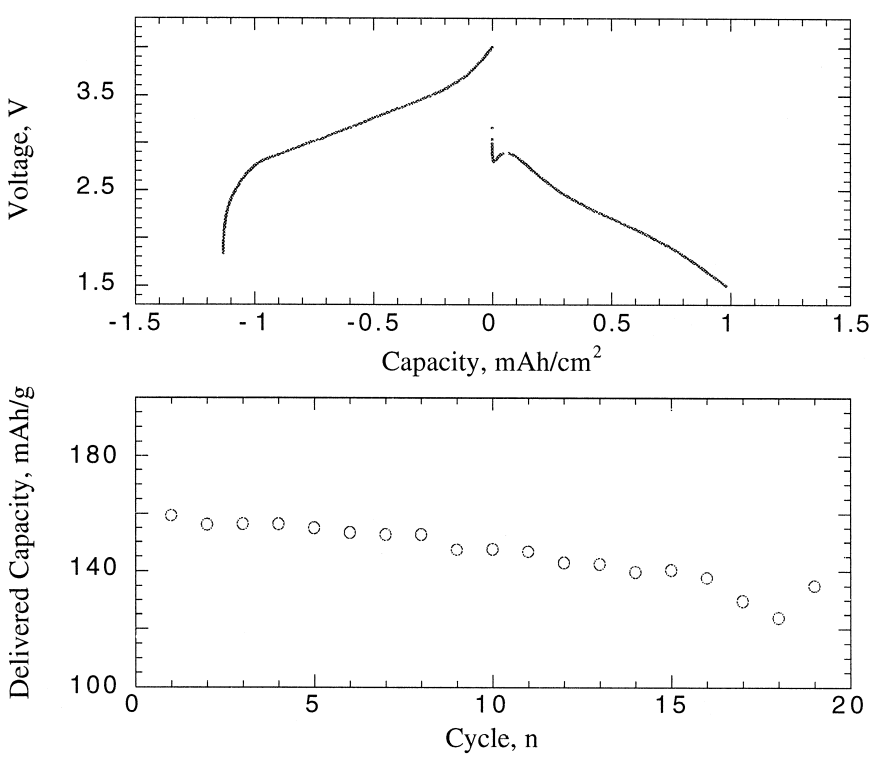

Fig. 13. Specific capacity upon galvanostatic cycles of the battery Li/EN20-20/VE20. Charge current: 0.08 mA/cm^2; discharge current: -0.17 mA/cm^2. $T = 90°C$.

reported as a function of the discharge current density (data are extracted from Fig. 10). As expected, the capacity delivered by the battery is seen to decrease as the discharge rate increased. The plot (Fig. 12) shows the existence of two regions of correlation between the delivered capacity and the current density. The low current region is characterized by a relation between the delivered capacity, called SC, and the inverse of the square root of the current density ($SC \propto i^{-0.5}$). In this region the delivered capacity is probably limited by the charge transfer at the polymer electrolyte–active material interface, as indicated by the very high value of the charge transfer resistance detected by impedance measurements (see comments of Fig. 9). Alternatively, a limitation by diffusion of lithium in the solid phase of the active material (V_2O_5 XRG) cannot be excluded. In the high current region, the capacity change linearly with the inverse of the current density ($SC \propto i^{-1}$). The latter relation is similar to the one seen previously for a symmetric Li/EN20-20/Li cell although the current values are smaller than the measured limiting current (i_L) in the polymer electrolyte. This apparent contradiction is simply explained considering that the bottleneck for the lithium diffusion in the battery is no longer located in the electrolyte region but in the composite cathode where the presence of the other cathode components reduces the cross-sectional area of the polymer electrolyte. If the composite cathode components are uniformly distributed it is possible to calculate the limiting current into the composite cathode (i_L^c). This will be given by the product of the limiting current into the polymer electrolyte (i_L) and the volumetric fraction of the latter in the composite cathode (see Section 2). In the specific case i_L^c is 0.07 mA/cm^2. In the results reported in Fig. 12, such a limit is never reached because of the appearance of a limitation due to the active material. Nevertheless, at the highest rates considered in this work, the delivered capacity of the battery was limited by the diffusion of the lithium into the polymer electrolyte fraction within the composite cathode.

Fig. 13 illustrates the cycling performances of a Li/EN20-20/VE20 battery. In the upper plot is shown a generic charge/discharge cycle. The discharge takes place in approximately 6 h and the recharge requires twice that time. The curve shows a quite large cell polarization, approximately 1 V, when the current is reversed. The lower plot shows the capacity delivered by the battery in the first 20 cycles. The initial value was 160 mA h/g that decreased slowly upon cycling. The slow decline of capacity has been seen before in V_2O_5 XRG composite cathodes in liquid electrolyte batteries [19,20] and the cause is not fully clear yet. Since thin, compact films of V_2O_5 XRG have shown very good cycling behavior [19,22,23], it has been proposed that the cause of the capacity fading in the composite pellets was the loss of contact between active material and carbon particles upon cycling [21]. The effect of the contact loss can be even more dramatic in the composite cathode used in present work since the contact between the active material and the electrolyte can also be lost upon cycling. Investigations on this issue are currently going on in our laboratories.

4. Conclusions

In this report were described the fabrication and the characterization of a lithium-metal, polymer electrolyte battery that uses V_2O_5 xerogel as cathode and operates at moderate temperature (80–100°C). The work has been focused on the determination of important 'application' properties of the polymer electrolyte, i.e., the properties of the polymer electrolyte in real systems and in true operating conditions.

First, it has been shown that processing that is characteristic of manufacturing gives a polymer electrolyte with improved performance. For example, its ionic conductivity at 60°C is about 10^{-4} S/cm. This value exceeds by more than one order of magnitude the conductivity of a polymer electrolyte with the same composition but prepared with laboratory equipment. The improvement is due to the optimization of the components in the mixture, in particular to the more uniform dispersion of the inert filler (γ-$LiAlO_2$).

The polymer electrolyte showed very good performance also in terms of stability and lithium cyclability at the lithium–polymer electrolyte interface. Impedance measurements have confirmed that there is good stability of such an interface under rest conditions. Lithium plating–stripping processes were seen to have a reversible character. As a matter of the fact, plating–stripping efficiency as high as 98% have been measured in operating conditions, i.e., when current flows through the electrolyte.

It has been proposed that a new criterion is necessary to establish the anodic stability of polymer electrolytes in contact with the carbon additive in composite cathodes. Depending on the carbon or the lithium salt used, anodic stabilities around 4.0 V (vs. Li) were measured in the present system. This value appears to allow the polymer electrolyte studied here to be used in combination with so-called '3 V' cathodic materials.

Galvanostatic pulse measurements have shown that the polymer electrolyte limiting current at 90°C is 0.2 mA/cm^2. If the current flowing through the electrolyte is larger than the limiting current, then the process can be sustained only for a finite time (τ) as predicted by the Sand equation. This implies that the delivered capacity of a battery containing a polymer electrolyte (either in the electrolyte layer or in the composite cathode) is limited by the time that the polymer electrolyte can sustain the current when the current is above the limiting current. At current densities below the limiting current, the delivered capacity is instead limited by the composite electrode. The design of a polymer electrolyte battery must consider these different limitations. High rate batteries can be realized

only by reducing the electrode thickness. The electrolyte thickness affects only the ohmic drop and not the delivered capacity.

Acknowledgements

The authors would like to thank all the participants to the ALPE project. In particular, Professor Bruno Scrosati for the useful discussions and Dr. G.B. Appetecchi and Dr. F. Ronci for kindly executing some electrochemical measurements. Work at the Corrosion Research Center was partially supported by DoE under the contract DE-FG02-93ER14384.

References

[1] A. Hooper, J.M. North, Solid State Ionics 9–10 (1983) 1161.
[2] M. Gautier, D. Fateaux, G. Vassort, A. Belanger, M. Duval, P. Ricoux, J.M. Chabagno, D. Muller, P. Rigaud, M.B. Armand, D. Deroo, J. Electrochem. Soc. 132 (1985) 1333.
[3] M. Armand, J.M. Chabagno, M.J. Duclot, in: P. Vashishita, J.N. Mundy, G.K. Shenoy (Eds.), Fast Ion Transport in Solids, Elsevier, New York, 1979, p. 131.
[4] F. Capuano, F. Croce, B. Scrosati, J. Electrochem. Soc. 138 (1991) 1918.
[5] M.C. Borghini, M. Mastragostino, S. Passerini, B. Scrosati, J. Electrochem. Soc. 142 (1995) 2118.
[6] G. Dautzemberg, ENEA Technical Report ALPE Project 1.2.2.1M, 1997.
[7] F. Alessandrini, F. Pallini, M. Carewska, P.P. Prosini, S. Passerini, ENEA Technical Report ALPE Project 6-97, 1997.
[8] D.B. Le, W.H. Smyrl, B.B. Owens, S. Passerini, U.S. Patent No. 5,674,642, 1997.
[9] F. Coustier, S. Passerini, W.H. Smyrl, J. Electrochem. Soc., 1998, accepted for publication.
[10] A.L. Tipton, S. Passerini, B.B. Owens, W.H. Smyrl, J. Electrochem. Soc. 143 (1996) 3473.
[11] J.E. Weston, B.C.H. Steele, Solid State Ionics 7 (1982) 75.
[12] S. Pantaloni, S. Passerini, F. Croce, B. Scrosati, Electrochim. Acta 34 (1989) 635.
[13] Southampton Electrochemistry Group, Instrumental Methods in Electrochemistry, Ellis Horwood, Chichester, UK, 1985.
[14] A.J. Bard, L.R. Faulkner, Electrochemical Methods, Wiley, New York, USA, 1980.
[15] B.A. Boukamp, Solid State Ionics 20 (1986) 31.
[16] G. Pistoia, A. Antonini, G. Wang, J. Power Sources 58 (1996) 139.
[17] M. Hiratani, K. Miyauchi, T. Kudo, Solid State Ionics 28–30 (1988) 1431.
[18] R.D. Armstrong, T. Dickinson, P. Willis, Electroanal. Chem. 53 (1974) 389.
[19] S. Passerini, D.B. Le, H.C. Foong, B.B. Owens, W.H. Smyrl, The Electrochemical Society Proceedings, PV 94-28, 1994, 297.
[20] K. West, B. Zachau-Christiansen, T. Jacobsen, S. Skaarup, Electrochim. Acta 38 (1993) 1215.
[21] A.L. Tipton, S. Passerini, B.B. Owens, W.H. Smyrl, J. Electrochem. Soc. 143 (1996) 3473.
[22] H.-K. Park, W.H. Smyrl, J. Electrochem. Soc. 141 (1994) L25.
[23] H.-K. Park, W.H. Smyrl, M.D. Ward, J. Electrochem. Soc. 142 (1995) 1068.